Journal of Mechanical Science and Technology 〈KSME I. J.〉 〈Special Edition〉 Vol. 19, No. 11, pp. 2105~2111, 2005

Contour Offset Algorithm (COA) in Nano Replication Printing (nRP) for Fabricating Nano-Precision Features

Tae Woo Lim, Sang Hu Park, Dong-Yol Yang*
Department of Mechanical Engineering, KAIST Daejeon, Korea
Shin Wook Yi, Hong Jin Kong
Department of Physics, KAIST Daejeon, Korea
Kwang-Sup Lee
Department of Polymer Science and Engineering, Hannam University Daejeon, Korea

A Contour Offset Algorithm (COA) has been developed to fabricate nano-precision figures or patterns in the range of several microns by a nano-Replication Printing (nRP) process. In the nRP process, a femtosecond laser illuminated on photosensitive monomer resin to induce polymerization of the liquid monomer according to a volume pixel (voxel) matrix which is transformed from a two-tone (black and white) bitmap file. After two-photon absorbed photopolymerization (TPP), a droplet of ethanol is dropt on a glass plate to remove the unnecessary remaining liquid resin, leaving only polymerized patterns on the glass plate. In the nRP process, the replicated patterns do not precisely coincide with the initial designs due to an essential shortage of nRP process. Fabricated patterns by means of the nRP process become larger than the design in the amount of the voxel radius. In this work, an outer contour matrix of an initial design was constructed and reduced according to an offset-ratio calculated by the COA in order to obtain more precise patterns. Both the effectiveness and the accuracy of the proposed algorithm were demonstrated through chosen example.

Key Words : Femtosecond Laser, Two Photon Polymerization, Contour Offset Algorithm (COA), Nano-replication Printing (nRP)

1. Introduction

Two-photon absorbed photopolymerization (TPP) has been recognized as one of the most promising technologies for producing more integrated and more diversified nanodevices, because it has the virtue of allowing the direct fabrication of nano-detailed two-dimensional patterns or true three-dimensional structures without any additional process. A unit volume (volume pixel ; voxel) size of several hundred nanometers for TPP induced by a femtosecond laser can be obtained without any actual restraint due to the diffraction limit of a beam. It has been recently reported that femtosecond laser pulses can be tightly focused onto liquid-state monomers and initiate a chemical process by TPP with feature sizes close to 100 nm (Nakamura, 1993). In TPP, a highly localized area around the center of a focused beam can be solidified by controlling the threshold energy for polymerization (Tanaka et al., 2002).

The nonlinear two-photon process has attracted a great deal of attention owing to its extensive potential in application fields such as a three-dimensional (3D) optical data storage, two-photon excited fluorescence for non-destructive bio-imaging, two-photon photodynamic therapy, 3D photonic crystals, and precision high resolu-

* Corresponding Author,
E-mail : dyyang@kaist.ac.kr
TEL : +82-42-869-3254; **FAX** : +82-42-869-3210
Department of Mechanical Engineering, KAIST Daejeon, Korea. (Manuscript **Received** January 25, 2005; **Revised** May 13, 2005)

tion laser microfabrication (Tanaka et al., 2002; Maruo et al., 1997; Maruo and Kawata, 1998; Sun et al., 1999; Galajda and Ormos, 2001; Serbin et al., 2003). True 3D microfabrication by TPP has been subject of particularly strong interest, because it provides a feasible approach to the fabrication of highly-integrated micro information storage devices. These devices evidently require high structural complexity, while the conventional photolithography has limitations for the fabrication of complex 3D structures.

Recently, the demand for ultra-precision technologies related with nanotechnology (NT), biotechnology (BT), and information technology (IT) has been dramatically increased for the development of the new conceptual and high-value-added products. In particular, cost-effective and mass-productive methodologies are in strong demand at present. Many studies have been devoted to advances in this area. Nano-imprinting (Chou et al., 2002) and soft-lithography (Xia and Whitesides, 1998) were introduced as cost-effective and simple processes, as well as being suitable for mass-production and diversified applications. However, these techniques suffer from several limitations. For example, the electron beam lithography-based process employed to fabricate master patterns in those processes is very expensive.

In this study, a nano Replication Printing (nRP) process has been developed. This process allows the direct fabrication of nano-precision patterns on a glass plate without a photomask by using TPP that is induced by a femtosecond laser. In this process, a voxel matrix scanning (VMS) scheme was introduced to scan along the x-axis and the y-axis to generate patterns on the plate, and the voxels were generated at the center position of the entities in a voxel matrix. As a result, however, the replicated patterns have undesirable shape-error factors; that is, they suffer from a false representation due to the size of the voxel. The voxel size of nRP process is about 200 nm which is large in comparison with the minimum feature size of SPM or E-beam lithography as shown in Table 1 (Myhra, 2004; Lehmann et al., 2003; Park et al., 2004; Lim et al., 2005; Goodberlet and Dunn, 2000; Sanjana and Fuller, 2004). Therefore, a contour offset algorithm (COA) is proposed to improve the limit of the nRP process and provide more precise patterns.

Table 1 Comparison of master pattern fabrications.

	Min. size (μm)	Aspect ratio	Throughput	Cost
nRP	~0.1	<10	middle	middle
SPM	0.01	<1	Low	High
E-beam	0.01	<1	Low	High
Photo-lithography	~1	<10	High	Low
Ink jet printing	>1	<1	High	Low

2. Nano Replication Printing Process

The resolution of the microstructures in the nRP process is determined by the size of a voxel. If the intensity distribution of a laser beam is assumed to be Gaussian, the geometric relations are given as follows;

$$\frac{r_c^2}{w_0^2} - \frac{z^2}{(b/2)^2} = 1 \qquad (1)$$

$$w_0 = \left(\frac{2\lambda f}{\pi d}\right),\ b = \frac{2\pi w_0^2}{\lambda} \qquad (2)$$

where w_0, f, d, b, and λ are beam waist, focal length, beam diameter, Rayleigh range, and wavelength, respectively, as shown in Fig. 1. Now, the intensity profile in the focal plane is

$$H(r) = H(0)\exp\left(\frac{-2r^2}{r_c^2}\right)$$
$$H(0) = \left(\frac{2}{\pi r_c^2}\right)P \qquad (3)$$

where $H(r)$ is the intensity of the laser per unit area, r_c denotes the radius of a beam contour, and P is laser power. The exposure energy of the laser for TPP can be expressed by eq. (4) as shown in the following, because the probability of TPP is proportional to the square of the laser intensity (Denk et al., 1990).

$$E(r, z, t) = \alpha\left[H(0)\exp\left(\frac{-2r^2}{r_c^2}\right)\right]^2 \cdot t \qquad (4)$$

where E is the exposure energy of the laser for time interval t and α is a proportional constant. Let the exposure energy of a laser (E) be the

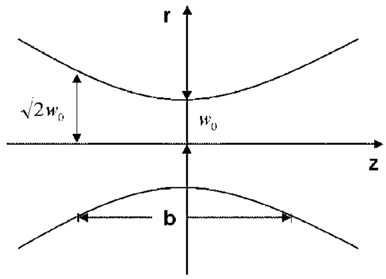

Fig. 1 The contour of Gaussian beam in the focal region.

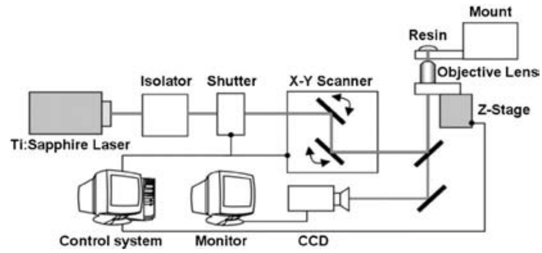

Fig. 2 Schematic diagram of an optical system for nRP process

threshold exposure energy (E_{th}) for TPA polymerization in eq. (4). The diameter of a voxel can then be given as eq. (5).

$$d(P, t) = 2r_{z=0} = w_0\left\{\ln\left(\frac{4P^2t}{\pi^2 w_0^4 E_{th}}\right)\right\}^{\frac{1}{2}} \quad (5)$$

In addition, the height, $l(r=0)$ of a voxel can be expressed as eq. (6).

$$l(P, t) = 2z_{r=0} = \frac{2\pi w_0^2}{\lambda}\left\{\left(\frac{4P^2t}{\pi^2 w_0^4 E_{th}}\right)^{\frac{1}{2}} - 1\right\}^{\frac{1}{2}} \quad (6)$$

The femtosecond laser system and the optical instruments for the nRP process are schematically shown in Fig. 2. The mode-locked Ti : Sapphire laser beam (780 nm wavelength, 80 MHz repetition, and 80 fs pulse width) is projected onto a Galvano-mirror type scanner (x-axis and y-axis scanner). An isolator and a shutter are located between the Ti : Sapphire laser and the scanner ; the former is applied to prevent the backward beam reflecting to the laser oscillator, and the latter is employed to control the beam on/off. The shutter could be generated up to 5 kHz, but 500 Hz response time is preferred for stable operation in this work. The beam was scanned on the focal plane by the scanner with a resolution of about 24 nm per step, and the focal plane was moved along the vertical axis using a piezo-stage.

In the nRP process, a raster graphics type of a voxel matrix, which consists of '0's for white pixels and '1's for black pixels transformed from a black-and-white bitmap image, was employed to scan the patterns on the glass plate. The laser beam was tightly focused with an objective lens (NA 1.25×100, immersion oil used) on the photopolymerizable resin, which was dropped on a cover-glass plate, as described above. Then, the laser focal spot was scanned on the glass plate by a computer controlled scanner with 24 nm resolution and by a piezoelectric z-stage with 100 nm resolution. Micro patterns were directly fabricated by a raster graphics type voxel matrix scanning (VMS) scheme, which is proposed to easily produce a 2D micro-pattern according to the entities of a voxel matrix ; in case of '1' elements in the voxel matrix, the shutter was open in order to generate photopolymerized voxels ; in the opposite case, the shutter was closed to prevent the generation of voxels.

When solidified by TPP, the remaining extra liquid-state monomer can be eliminated easily after dropping several ethanol droplets on the patterns. The imaging system, which employs a high magnifying CCD camera, is useful for optical adjustment. In addition, the status of fabrication progress can be monitored in real-time by the imaging system, as shown in Fig. 2.

The Two-photon Absorption (TPA) material used in the work was a mixture of urethane acrylate monomers and photo-initiators. The density of the photo-initiator is 0.1%(w/w). The absorption and fluorescence spectrums of the photo-initiator are 411 nm and 472 nm, respectively : The photo-initiator absorbs 411 nm wavelength light and emits 472 nm wavelength light. Radicals are activated when the 472 nm light is illuminated.

3. Process Parameters of the nRP Process

The resolution of a fabricated pattern is related to the size of a voxel. The voxel dimensions are obtained by eqs. (5) and (6), and the laser power and the exposure time are major parameters to determine the dimensions of a voxel. In this work, several experiments were attempted to minimize the voxel size with respect to the variation of process parameters, and the results of the experiments were matched qualitatively to the theoretical prospects.

The lowest laser power for TPP was estimated as 2 mW in preliminary tests, but the fabricated voxels at that power were not stable with various exposure times. Irregular and distorted voxels were fabricated when the laser power was greater than 6 mW. In this work, a laser power of 5 mW was estimated as a stable condition to fabricate voxels with various exposure times. From the experiments, the minimum voxel diameter was approximately 200 nm for an exposure time of 2 ms and the laser power of 5 mW.

A contour offset algorithm (COA) was proposed to improve the precision of the patterns fabricated by the nRP process. Fig. 3 shows an Extra shape of a fabricated pattern. The shape-error term in the fabricated pattern should be eliminated to improve its degree of precision, and the amount of a shape-error term for modification of the original contour of the designed bitmap file can be calculated by the ratio of the voxel radius to the total pattern size.

In the proposed algorithm, the modification process is as follows; first, a contour matrix is extracted from an original voxel matrix, which is transformed from the original bitmap file. Then, the outer contour matrix is converted into a commercial CAD data format such as an I-DEAS importing format in order to offset it in the CAD system.

The offset-amount (R_{offset}) in the CAD system can be calculated by the following relation:

$$R_{offset} = (L \times r)/l \qquad (7)$$

where L, r, and l denote the total size of a pattern in the CAD system, the voxel radius, and the total size of a fabricated pattern, respectively. The parameters L and r are known variables; specifically, they are, respectively, the total size of the original bitmap figure and the voxel radius that is obtained by preliminary experiments. And the total fabricated pattern size (l) can be simply calculated by using the voxel matrix, the distance between voxels, and the voxel diameter. The total size of the fabricated pattern is dependent on the voxel matrix size which is determined by the size of the bitmap figure. Thus, the fabricated pattern size can be controlled by enlarging or reducing the original bitmap figure. After modification of the outer contour, a new matrix is reconstructed from the modified bitmap file. A flowchart of the COA process is shown in Fig. 4.

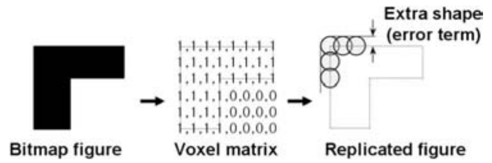

Fig. 3 Replication process and extra shape term.

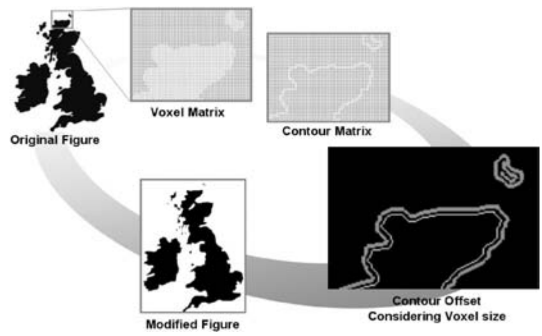

Fig. 4 Schematic diagram of Contour Offset Algorithm.

4. Direct Patterning by the Contour Offset Algorithm

To estimate the effectiveness of the COA, a standard doughnut-shaped test-specimen, which consists of an inner and an outer contour with the ratio of the radii (inner vs. outer contour; 1 to 2), has been fabricated with and without the COA, as shown in Fig. 5. The offset-amount (R_{offset}) of the standard test-specimen was calculated as 1.27 mm by eq. (7) for the given data, i.e., L (diameter of the outer contour in CAD program ; 100 mm), r (radius of voxel ; 100 nm), and l (diameter of the outer contour to be fabricated ; 7.9 μm). For the case where COA was not

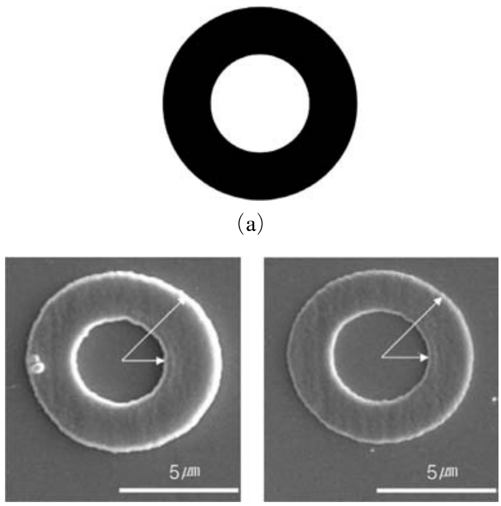

(a)

(b) (c)

Fig. 5 (a) Bitmap image of a standard test-specimen. (b) SEM image of replicated patterns without the COA, and (c) with the COA.

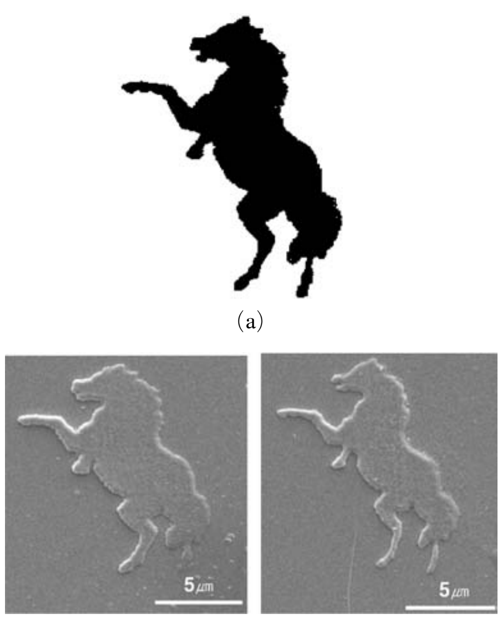

(a)

(b) (c)

Fig. 6 SEM images of the replicated figures ; (a) an original bitmap figure of a horse, (b) its replicated figure without the COA, and (c) with the COA.

applied, the ratio of the inner radius to the outer radius of the replicated doughnut was 1 to 2.11 ; however when the COA was employed, the ratio was 1 to 1.97.

Furthermore, the shape error-terms in the fabricated pattern were reduced from 5.5% to 1.5%. Thus, the figure replicated by the COA was more precise as compared with the case without the COA.

To evaluate the usefulness of the COA, complicated patterns such as a map of England and a horse were fabricated with and without the COA. For the map of England bitmap figure, the offset-amount (R_{offset}) was calculated to be 0.82 mm for the following conditions : L (longitudinal length of the image in CAD program ; 125 mm), r (radius of voxel ; 100 nm) and l (longitudinal length of the image to be fabricated ; 15.2 μm). For horse, the offset-amount (R_{offset}) was 0.83 mm for l (123 mm), r (100

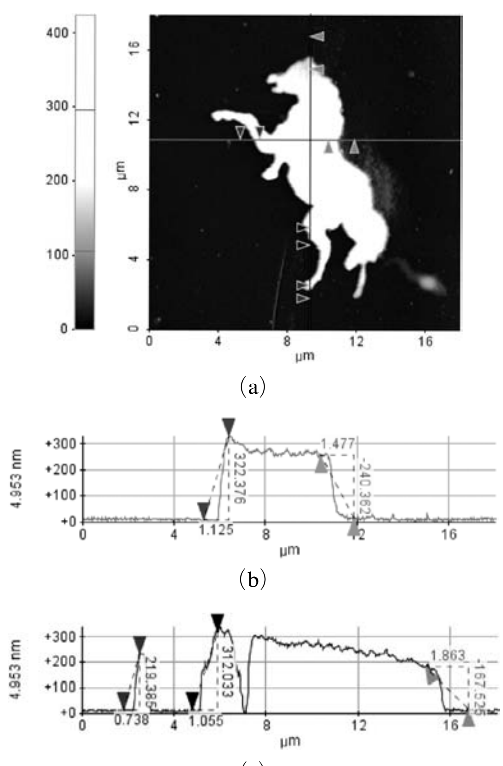

(a)

(b)

(c)

Fig. 7 (a) AFM image of a horse, (b) profile of the height along the lateral line, and (c) along the longitudinal line nm), and l (14.9 μm).

As shown in Fig. 6, the COA is a very effective algorithm to improve the precision of replicated figures in the nRP process. Fig. 7 shows an AFM (PSIA, XE-100) image of the fabricated horse pattern. The pattern is flat and the height is about 300 nm. However, the center of the pattern is slightly higher than the outer region because of the difference of the laser power entering the objective lens. Almost all of the laser power is transmitted through the objective lens when the center of the pattern is scanned, but the laser power to be transmitted through the objective lens is reduced when the outer region of the pattern is scanned. Thus, the flatness can be improved by expanding the laser beam, and the flatter surface consisting of uniform voxels will be fabricated.

Various patterns with high precision by using COA can be fabricated via the nRP process, and they can be used as master patterns in the processes, nano imprinting, as or soft-lithography, etc.

5. Conclusions

Two-photon absorbed photopolymerization (TPP) provides a means to directly fabricate nano-detailed patterns in a cost-effective manner. In this study, a two-dimensional figure with a resolution of 200 nm was fabricated by the nano replicating printing (nRP) process. In the process, a voxel matrix scanning (VMS) scheme with raster graphics type allowed the fabrication of two-dimensional micro-patterns from a bitmap format figure. The shape error-terms due to the intrinsic problems of the VMS scheme could be eliminated by the COA. The effectiveness of the COA was evaluated through the fabrication of a standard test-specimen, a horse and a map of England, with and without the COA. Thus, It could be confirmed that the COA is an integral process in every additional processes of nRP process which need 2D master patterns.

Acknowledgment

The research work was funded by the Center for Nanoscale Mechatronics & Manufacturing of the 21st Frontier Project Supported by Korean Ministry of Science & Technology.

References

Chou, S. Y., Keimel, C. and Gu, J., 2002, "Ultrafast and Direct Imprint of Nanostructures in Silicon," *Nature*, Vol. 417, No. 20, pp. 835～837.

Denk, W., Strickler, J. H. and Webb, W. W., 1990, "Two-Photon Laser Scanning Fluorescence Microscopy," *Science*, Vol. 248, pp. 73～248.

Galajda, P. and Ormos, P., 2001, "Complex Micromachines Produced and Driven by Light," *Appl. Phys. Lett*., Vol. 78, No. 2, pp. 249～251.

Goodberlet, J. G. and Dunn, B. L., 2000, "Deep-Ultraviolet Contact Photo-lithography," *Microelectronic Engineering*, Vol. 53, pp. 95～99.

Lehmann, F., Richter, G., Borzenko, T., Hock, V., Schmidt, G. and Molenkamp, L. W., 2003, "Fabrication of Sub-10-nm Au-Pd Structures using 30keV Electron Beam Lithography and Lift-off," *Microelectronic Engineering*, Vol. 65, pp. 327～333.

Lim, T. W., Park, S. H. and Yang, D.-Y., 2005, "Contour Offset Algorithm for Precise Patterning in Two-photon Polymerization," *Microelectric Engineering*., Vol. 77, pp. 382～388.

Maruo, S. and Kawata, S., 1998, "Two-photon-absorbed Near-infrared Photopolymerization for Three-dimensional Microfabrication," *J. of Microelectromechanical Systems*, Vol. 7, No. 4, pp. 411～415.

Myhra, S., 2004, "Manipulation of Si Oxide and Electrically Conducting Carbon Films by Scanning Probe Microscopy (SPM): Nano-lithography and Nano-machining," *Thin Solid Films*., Vol. 459, pp. 90～94.

Nakamura, O., 1993, "Three-dimensional Imaging Characteristics of Laser Scan Fluorescence Microscopy : Two-photon Excitation Vs. Single-photon Excitation," *Optik*, Vol. 93, No. 1, pp. 39～41.

Park, S. H., Lim, T. W., Yol, D.-Y. and Kong, H. J., 2004, "Fabrication of a PDMS (Poly-Dimethylsiloxane) Stamp using Nano-replication

Printing Process," *J. of KSME* (*A*), Vol. 28, No. 7, pp. 999~1005.

Sanjana, N. E. and Fuller, S. B., 2004, "A Fast Flexible Ink-jet Printing Method for Patterning Dissociated Neurons in Culture," *J. Neuroscience Method*, Vol. 36, pp. 151~163.

Serbin, J., Egbert, A., Ostendorf, A., Chichkov, B. N., Houbertz, R., domann, G., Schulz, J., Cronauer, C., Frohlich, L. and Popall, M., 2003, "Femtosecond Laser-induced Two-photon Polymerization of Inorganic-organic Hybrid Materials for Applications in Photonics," *Opt. Lett.*, Vol. 28, No. 5, pp. 301~303.

Sun, H.-B., Matsuo, S. and Misawa, H., 1999, "Three-dimensional Photonic Crystal Structures Achieved with Two-photon-absorption Photopolymerization of Resin," *Appl. Phys. Lett.*, Vol. 74, No. 6, pp. 786~788.

Tanaka, T., Sun, H.-B. and Kawata, S., 2002, "Rapid Sub-diffraction-limit Laser Micro/nanoprocessing in a Threshold Material System," *Appl. Phys. Lett.*, Vol. 80, No. 2, pp. 312~314.

Xia, Y. and Whitesides, G. M., 1998, "Soft Lithography," *Angew. Chem. Int. Ed.*, Vol. 37, pp. 550~575.

Maruo, S., Nakamura, O. and Kawata, S., 1997, "Three-dimensional Microfabrication with Two-photon-absorbed Photopolymerization," *Opt. Lett.*, Vol. 22, No. 2, pp. 132~134.